

Three-dimensional recording by tightly focused femtosecond pulses in LiNbO₃

Saulius Juodkazis,^{a)} Markas Sudzius, Vyngantas Mizeikis, and Hiroaki Misawa^{b)}
 CREST-JST, Research Institute for Electronic Science, Hokkaido University, CRIS Bldg. N21-W10,
 Sapporo 001-0021, Japan

Eugene G. Gamaly
 Laser Physics Centre, Research School of Physical Sciences and Engineering,
 The Australian National University, Canberra, Australian Capital Territory 0200, Australia

Youwen Liu, Oleg A. Louchev, and Kenji Kitamura
 Optronics Materials Center, National Institute for Materials Science, 1-1 Namiki, Tsukuba 305-0044, Japan

(Received 14 March 2006; accepted 18 June 2006; published online 7 August 2006)

The authors report on a three-dimensional single-shot optical recording by 150 fs pulses at 800 nm wavelength in Fe doped LiNbO₃. The rewritable bits ($2_x \times 2_y \times 8_z \mu\text{m}^3$) are demonstrated. The highest refractive index modulation of $\sim 10^{-3}$ per single pulse has been formed by preferential photovoltaic effect at close to the dielectric breakdown irradiance of $\sim \text{TW}/\text{cm}^2$ and was independent of polarization (in respect to the c axis). The achievable refractive index modulation is evaluated and the recording mechanisms are discussed. © 2006 American Institute of Physics. [DOI: 10.1063/1.2335364]

Nonlinear optical crystals LiNbO₃ have a very wide field of applications including three-dimensional (3D),¹ holographic optical memory,^{2,3} and photonic crystals.⁴ The photorefractive mechanisms of a photoinduced space-charge field E_{sc} formation, which induce corresponding refractive index modulation via the electro-optical effect,⁵ are well understood at weak continuous wave (cw) or pulsed laser exposure.^{6,7} The buildup of E_{sc} field is a result of electron diffusion and retrapping, hence limiting the overall rate of recording. Usually, a prolonged exposure of hologram by cw or pulsed illumination is necessary to achieve a high efficiency of diffraction for high fidelity readout. The stability of the recorded structures is limited by the dark-current conductivity and photoconductivity. The thermal fixing provides the best results for optically nonerasable memories.⁸

Here, we show formation of a micrometer-sized domain of a high refractive index modulation ($\sim 10^{-3}$) predominantly via a photovoltaic effect by a single-pulse exposure. The contributions of diffusion, pyroelectric, and photovoltaic mechanisms of refractive index modulation at high irradiance ($\sim \text{TW}/\text{cm}^2$) have been estimated.

Single near-stoichiometric (Li/Nb=49.85/50.15) 400 ppm Fe doped crystals (Y cut) [Fig. 1(a)] were used in this study due to larger photo-refractive sensitivity than the conventional congruent LiNbO₃.⁹ The laser source (Hurricane, Spectra Physics) was delivering 150 fs pulses of 800 nm wavelength at repetition rate of 1 kHz. The thresholds for recording of optically recognizable modification (visualized through the refractive index modulation in the vicinity of the focal spot) were 3.8 ± 0.5 nJ in LiNbO₃:Fe and 5.2 ± 0.5 nJ in undoped LiNbO₃ (a reference sample), respectively, for focusing by an objective lens of numerical aperture NA=0.55 at a 50 μm depth. In order to minimize the spherical aberration, the divergence of the laser beam was

tuned for the smallest value of the breakdown and the smallest cross section of photomodification site. The aberration free focusing of a plane wave would correspond to the waist (radius) $w_0 = 0.61\lambda/\text{NA} \approx 0.88 \mu\text{m}$ (at a $1/e^2$ -intensity level), while the full width at half maximum (FWHM) radius would be smaller by a factor of $\sqrt{\ln(2)/2}$. The diameter of the bit formed by a single 7 nJ pulse was approximately 1.1 μm (FWHM) as observed in microscope with a higher NA=1.35 objective lens. This is close to the expected focal FWHM cross section. Permanent structural damage occurred at 11–12 nJ pulse energy as a result of dielectric breakdown causing the largest refractive index modulation observed. Hence, the formation of refractive index modulation at high irradiance $I = 6.7 \text{ TW}/\text{cm}^2$ (fluence $F = 1 \text{ J}/\text{cm}^2$), which corresponds to a 10 nJ pulse of 150 fs with the waist of $r_0 = 0.55 \mu\text{m}$, was considered in the modeling of light-matter interaction. The axial extent of the photomodified volume, the Rayleigh length, was $z_0 = \pi w_0^2 n / \lambda \approx 6.8 \mu\text{m}$; here $n = 2.2$ is the real part of the refractive index in LiNbO₃.

Figure 1 shows a 3D recording (b) and rewriting [(c) and (d)] of photomodified regions, voxels, in LiNbO₃:Fe at 10 μm depth. Rewriting was confirmed by recording different patterns [bottom upwards in (c)]: (i) line of voxels at 0.5 μm separation, (ii) same line passing over a single pre-recorded bit, (iii) a single bit recorded after procedure (i), and (iv) a single bit. The resulting pattern after 20 and more cycles of rewriting is shown in (d). When polarization of recording and imaging was perpendicular to the c axis, the highest contrast resulted (Fig. 1). The observed optical modulation and contrast are consistent with a space-charge field pattern generated via photovoltaic effect.^{10,11} It is noteworthy that there was no polarization dependence of the voxel contrast on polarization of recording.¹¹ This is different from femtosecond multipulse recording,¹⁰ most probably, due to considerably smaller spot size in our experiments. The brighter regions (Fig. 1) correspond to the refractive index increase and vice versa.¹¹ An inverted optical contrast was

^{a)}Electronic mail: saulius@es.hokudai.ac.jp

^{b)}Electronic mail: misawa@es.hokudai.ac.jp

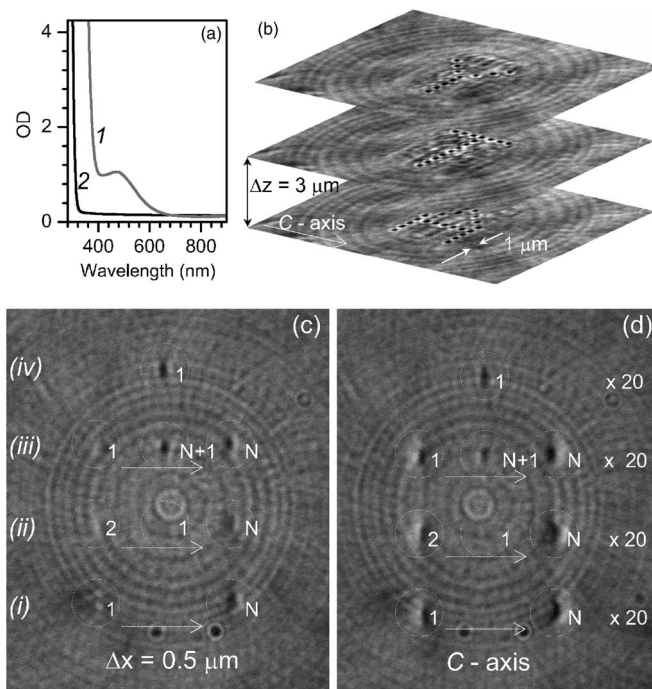


FIG. 1. (a) Absorption spectra of a 2-mm-thick Fe-doped (1) and undoped (2) LiNbO₃. (b) Layered recording of bits forming letters A, T, and Y using objective lens of numerical aperture NA=1.4, plane separation 3 μm, and pulse energy 6 nJ. (c) Transmission images of bits created by a single-pulse irradiation at 10 μm depth in a single crystal of LiNbO₃:Fe by 7 nJ pulses (NA=0.55). Irradiation sequence is marked by 1, 2, ..., N, see text for details. (d) Same as (c) only rewritten 20 times. Polarization of writing and reading was perpendicular to the *c* axis. Scale bar is 10 μm.

observed, similarly as in Ref. 11 in a nonpolarized imaging of recorded bits (Fig. 2).

A complete erasing of the recorded voxel was achieved by $a < 0.6 \mu\text{m}$ *c*-axis-shifted irradiation (Fig. 2). This type of erasing leaves a recognizable features at the start and stop positions. Thus, if a single voxel should be deleted from a line, a special sequence of voxels should be irradiated. However, this can be incorporated into the actual 3D optical memory application if required. Hence, the writing, erasing, and rewriting at the same wavelength by single pulses have been demonstrated. Since an effective recording of refractive index modulation occurs along the *c* axis, a 3D stacking of voxels' planes is possible in LiNbO₃. A high refractive index of LiNbO₃, $n=2.2878$ (o ray) 2.189 (e) (at $\lambda < 0.63 \mu\text{m}$), introduces a spherical aberration when focused at increasing

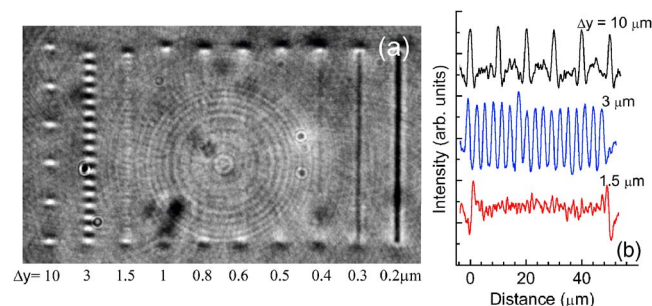


FIG. 2. (Color online) (a) Transmission image of voxels recorded by a single-pulse irradiation at 50 μm depth in LiNbO₃:Fe. Polarization of recording was vertical (along the *c* axis), imaging nonpolarized; separation Δy between pulses is marked at each line. (b) Cross section of the transmission along several recorded lines.

depth; however, this problem can be alleviated by usage of afocal optics (control of divergency of the laser beam).

The refractive index modulation was estimated by measuring the diffraction efficiency of $\Lambda=3 \mu\text{m}$ gratings recorded with the grating vector parallel to the *c* axis (no erasing). The distance between the adjacent voxels was $0.2 \mu\text{m}$. A high diffraction efficiency of the He-Ne laser, $\eta=I_1/I_T \approx (\pi\Delta n d/\lambda)^2 \approx 2\%$, was observed, which roughly corresponds to the refractive index modulation of $\Delta n \approx 6 \times 10^{-3}$; $I_{1,T}$ are the intensities of the diffracted and transmitted beams, respectively, $d \approx z_0 = 6.8 \mu\text{m}$ is the thickness of grating, and $\lambda = 633 \text{ nm}$ is the wavelength of readout. The high value of refractive index change and the possibility to form it by a single pulse of high intensity are demonstrated experimentally. We discuss below the contribution of different mechanisms and the maximum refractive index modulation at a prebreakdown exposure by a single pulse.

The light-matter interaction relevant to the employed high irradiance (intensity) is considered theoretically; the avalanche and multiphoton absorption rates are estimated. The gain of net energy via electron-lattice collisions by an electron oscillating in the electromagnetic field of the laser beam, Joule heating, can be calculated by

$$\frac{d\epsilon_e}{dt} \approx 2\epsilon_{\text{osc}} \frac{\omega^2 \nu_{e\text{-ph}}}{(\nu_{e\text{-ph}}^2 + \omega^2)} \approx 2\epsilon_{\text{osc}} \nu_{e\text{-ph}}, \quad (1)$$

where $\nu_{e\text{-ph}}$ is the electron-phonon collision rate, ϵ_{osc} the quiver energy of electron, and ω the cyclic frequency of light. The electron-phonon collision rate can be estimated in two ways. First, starting from the known heat diffusion, $D = 1.5 \times 10^{-2} \text{ cm}^2/\text{s}$, and using $D \approx v_s^2/(3\nu_{e\text{-ph}})$ with the assumption that sound velocity is $v_s = 4 \text{ km/s}$, one obtains $\nu_{e\text{-ph}} = 3.5 \text{ THz}$. Also, the phonon frequency can be estimated as the sound velocity divided by the interatomic distance ($5.148\text{--}13.865 \text{ \AA}$), i.e., $\nu_{e\text{-ph}} = 8\text{--}2.9 \text{ THz}$. The value $\nu_{e\text{-ph}} = 5 \text{ THz}$ will be used in further calculations. The electron oscillation energy in the laser field for a linearly polarized wave reads (in a scaling form) $\epsilon_{\text{osc}} = 9.3\Lambda^2 [\text{eV}]$, where I is in 10^{14} W/cm^2 and λ in micrometers. By taking $I = 6.7 \text{ TW/cm}^2$, one gets $\epsilon_{\text{osc}} = 0.4 \text{ eV}$. Then, for a $\nu_{e\text{-ph}} = 5 \text{ THz}$, one obtains the electron energy gain rate of $2 \times 10^{12} \text{ eV/s}$ and ionization rate by the avalanche process $w_{\text{av}} \approx (1/\Delta_{\text{gap}})(d\epsilon_e/dt) \sim 0.5 \text{ THz}$. Hence, the avalanche cannot produce sufficient number of conductivity electrons to the end of a 150 fs pulse by transferring them from valence to conduction band, $w_{\text{av}} t_p = 0.075$. However, the electron energy is sufficient for excitation of electrons from impurity levels located less than 0.4 eV below the edge of conduction band.

It is reasonable to take the ionization probability (per atom per second) in the multi-photon form: $w_{\text{mpi}} \approx \omega_{\text{ph}}^{3/2} (\epsilon_{\text{osc}}/2\Delta_{\text{gap}})^{n_{\text{ph}}}$; here $n_{\text{ph}} = \Delta_{\text{gap}}/\hbar\omega \sim 4/1.55 \text{ eV} = 2.575$ is the number of photons necessary for electron to be transferred from valence to the conductivity band. Taking $\omega = 2.356 \text{ fs}^{-1}$ and band gap $\sim 4 \text{ eV}$, one gets $w_{\text{mpi}} \approx 4.9 \times 10^{15} (I/10^{14})^{2.575} \text{ s}^{-1}$. Assuming flat-top-hat intensity distribution and taking $I = 6.7 \text{ TW/cm}^2$, one gets $w_{\text{mpi}} = 4.65 \text{ THz} \gg w_{\text{av}}$. For the Gaussian pulse with same maximum amplitude value I , the ionization rate should be reduced by $2\sqrt{n_{\text{ph}}} = 3.19$ times yielding in $w_{\text{mpi}} = 1.46 \text{ THz}$. Therefore, the number of conductivity electrons produced by a multiphoton process to the end of 150 fs pulse

is $n_e = w_{\text{mpi}} n_a t_p = 2 \times 10^{22} \text{ cm}^{-3}$ (the atomic density $n_a = 9.45 \times 10^{22} \text{ cm}^{-3}$), well in excess of the critical density $n_{\text{cr}} = 1.76 \times 10^{21} \text{ cm}^{-3}$ at 800 nm wavelength.

Let us suggest that the number of excited electrons equals the critical density to the end of the pulse and $\omega_{\text{pe}} \sim \omega \gg \nu_{\text{e-ph}}$. Then, the real part of the dielectric function will remain almost unchanged, $\epsilon \sim n^2$, while the imaginary part responsible for absorption is $\epsilon'' \approx \nu_{\text{e-ph}}/\omega$. The imaginary part of the refractive index expresses as $\kappa \approx \epsilon''/2n_0 = \nu_{\text{e-ph}}/2n_0\omega = 5 \times 10^{-4}$ (with $n=2.2$). Then, the absorption length (for an E field) becomes $l_s = c/\kappa\omega = 250 \mu\text{m}$.

The electron energy can be estimated by the following equation with the energy losses due to interaction with a lattice and heat conduction are neglected:

$$\frac{\partial C_e n_e T_e}{\partial t} = \frac{2A}{l_{\text{abs}}} I(r, z, t), \quad (2)$$

where A is the absorbance, l_{abs} is the absorption length, C_e the specific heat capacity per electron, T_e the electron temperature, and n_e the electron density. The estimate of the temperature to the end of laser pulse then reads

$$T_e \approx \frac{2A I t_p}{C_e n_e l_{\text{abs}}}. \quad (3)$$

One can estimate the electron temperature rise considering that the electrons are degenerate with $C_e = (\pi^2/2)(T_e/\epsilon_F)$. For $n_e \approx n_{\text{cr}} \sim 10^{21} \text{ cm}^{-3}$, $A \sim 2z_0/l_s$, $l_s \sim 2.5 \times 10^{-2} \text{ cm}$, $F \equiv I t_p = 1 \text{ J/cm}^2$, $z_0 = 2.9 \mu\text{m}$, and the Fermi energy $\epsilon_F \sim 10 \text{ eV}$, one gets $T_e^2 \approx (8z_0 I t_p / \pi^2 l_s^2 n_e) \epsilon_F$. To the end of the 150 fs pulse, the electron temperature comprises $T_e = 0.2 \text{ eV}$. Electrons transfer the absorbed energy to the lattice during the time $t_{e-L} \approx \nu_{\text{e-ph}}^{-1} \sqrt{M/m^*}$. For the average mass of atom $M = 29.6 \text{ a.u.}$ and free electron mass m^* , one finds $t_{e-L} = 4.6 \times 10^{-11} \text{ s}$. The total absorbed energy per volume reads $E_{\text{abs}} \approx 2A \cdot I \cdot t_p / l_{\text{abs}} \sim 1.85 \text{ J/cm}^3$. Thus, the temperature rise $\Delta T \approx 0.6 \text{ K}$ in a lattice is negligible [specific heat capacity $c_p = 628 \text{ J/(kg K)}$]. This implies that contribution of pyroelectric effect in buildup of E_{sc} was not effective in the considered case.

The contribution from diffusion and photovoltaic fields is considered next. The diffusion field reads $E_{\text{dif}} \approx (T_e/e) \times (\nabla n_e/n_e)$; here e is the electron charge. Taking $T_e \sim 0.2 \text{ eV}$ (at pulse end) and $\nabla n_e/n_e \propto w_0^{-1} \sim 2 \times 10^4 \text{ cm}^{-1}$ (in the plane of c axis), one gets moderate field of $E_{\text{dif}} \sim 3.6 \text{ kV/cm}$. This field decays along with the temperature decrease and smoothing the gradients due to the electron-lattice energy exchange and heat conduction.

The photovoltaic current j_{ph} can be excited in noncentrosymmetric medium due to laser excitation

$$j_{\text{ph}} = l_{\text{abs}}^{-1} G I, \quad (4)$$

where G is the Glass constant. If the laser beam is incident in the direction perpendicular to the c axis in LiNbO_3 , then the photovoltaic current is excited in the c direction. The quasi-

steady electric field is $E_{\text{ph}} = j_{\text{ph}}/\sigma$. The real part of the conductivity during the laser pulse action reads

$$\sigma = \frac{e^2 \cdot n_e \cdot \nu_{\text{e-ph}}}{m_e^* (\omega^2 + \nu_{\text{e-ph}}^2)}. \quad (5)$$

The conductivity in the absence of laser field (after the pulse end) takes the form $\sigma \approx e^2 n_e / m_e^* \nu_{\text{e-ph}}$. In the considered case, when $\omega_{\text{pe}} \sim \omega \gg \nu_{\text{e-ph}}$, one can present Eq. (5) in the form $\sigma \approx \nu_{\text{e-ph}}/4\pi \sim 0.4 \text{ THz}$. Now taking $G_{33} = 3 \times 10^{-9} \text{ cm/V}$ with the use of Eq. (4), one obtains $E_{\text{ph}} = 1.62 \text{ MV/cm}$, obviously the strongest effect from the all discussed.

The change in the refractive index due to presence of the field of the charge separation reads¹¹

$$\Delta n = -\frac{n^3 r}{2} E_{\text{sc}}. \quad (6)$$

For LiNbO_3 the ratio $\lambda/n^3 \cdot r = U_{\pi} \approx 2 \text{ kV}$ for $\lambda = 630 \text{ nm}$, corresponding for 800 nm, one gets $n^3 \cdot r \approx 6.35 \times 10^{-8} \text{ cm/V}$ (r is the electro-optic coefficient). Therefore, the theoretically achievable change of the refractive index is $|\Delta n| = 5.14 \times 10^{-2}$ at the pre breakdown irradiance of $I = 6.7 \text{ TW/cm}^2$. The calculated value is a theoretical maximum and it is, most probably, overestimated because the electron-phonon collision frequency in LiNbO_3 is not measured directly but is calculated. In our experiments, the optical contrast shown in Figs. 1(c) and 1(d) corresponds to the refractive index modulation approximately five times lower than the maximum estimate for a single pulse exposure.

In conclusion, a rewritable 3D optical memory has been demonstrated with refractive index modulation up to 6×10^{-3} . This large change can be recorded by a single femtosecond laser pulse using a dry objective lens proving an application potential. The photovoltaic mechanism accounts for the upper-bound estimate of achievable refractive index change by a single femtosecond laser pulse.

The authors are grateful to W. Krolikowski for critical remarks. One of the authors (M.S.) thanks the Matsumae International Foundation for the research fellowship. Another author (E.G.G.) acknowledges support of the Australian Research Council through its Center of Excellence.

¹Y. Kawata, H. Ishitobi, and S. Kawata, *Opt. Lett.* **23**, 756 (1998).

²M. Lee, S. Takekawa, Y. Furukawa, K. Kitamura, and H. Hatano, *Phys. Rev. Lett.* **84**, 875 (2000).

³L. Arizmendi, *Phys. Status Solidi A* **201**, 253 (2004).

⁴G. Zhou and M. Gu, *Appl. Phys. Lett.* **87**, 241107 (2005).

⁵*Photorefractive Materials and Their Applications I: Fundamental Phenomena*, Topics in Applied Physics, Vol. 61, edited by P. Günter and J.-P. Huignard (Springer, Berlin, 1988), pp. 7–98.

⁶K. Buse, *Appl. Phys. B: Lasers Opt.* **64**, 273 (1997).

⁷K. Buse, *Appl. Phys. B: Lasers Opt.* **64**, 391 (1997).

⁸T. Volk and M. Wöhlecke, *Crit. Rev. Solid State Mater. Sci.* **30**, 125 (2005).

⁹K. Kitamura, Y. Furukawa, Y. Ji, M. Zgonik, C. Medrano, G. Montemezzani, and P. Guenter, *J. Appl. Phys.* **82**, 1006 (1997).

¹⁰F. S. Chen, *J. Appl. Phys.* **40**, 3389 (1969).

¹¹O. Beyer, I. Breunig, F. Kalkum, and K. Buse, *Appl. Phys. Lett.* **88**, 051120 (2006).